

H - T phase diagram and the nature of Vortex-glass phase in a quasi two-dimensional superconductor: Sn metal layer sandwiched between graphene sheets

Masatsugu Suzuki^a Itsuko S. Suzuki^a Jürgen Walter^b

^a*Department of Physics, State University of New York at Binghamton,
Binghamton, New York 13902-6016, U.S.A.*

^b*Department of Materials Science and Processing, Graduate School of
Engineering, Osaka University, 2-1, Yamada-oka, Suita, 565-0879, JAPAN*

Abstract

The magnetic properties of a quasi two-dimensional superconductor, Sn-metal graphite (MG), are studied using DC and AC magnetic susceptibility. Sn-MG has a unique layered structure where Sn metal layer is sandwiched between adjacent graphene sheets. This compound undergoes a superconducting transition at $T_c = 3.75$ K at $H = 0$. The H - T diagram of Sn-MG is similar to that of a quasi two-dimensional superconductors. The phase boundaries of vortex liquid, vortex glass, and vortex lattice phase merge into a multicritical point located at $T^* = 3.4$ K and $H^* = 40$ Oe. There are two irreversibility lines denoted by H_{gl} (de Almeida-Thouless type) and $H_{gl'}$ (Gabay-Toulouse type), intersecting at $T'_0 = 2.5$ K and $H'_0 = 160$ Oe. The nature of slow dynamic and nonlinearity of the vortex glass phase is studied.

Key words: vortex glass phase, phase diagram, magnetic irreversibility

PACS: 74.25.Ha, 74.25.Dw, 74.60.Ec, 74.80.Dm

1 Introduction

The existence of vortex glass phase in the mixed state of quasi two-dimensional (2D) high- T_c superconductors such as $\text{YBa}_2\text{Cu}_3\text{O}_7$ in the presence of magnetic field (H) attracts considerable attention [1,2,3]. Müller et al. [4] have pointed out for the first time the existence of the glassy phase in $\text{La}_2\text{CuO}_{4-y}\cdot\text{Ba}$. They

Email address: suzuki@binghamton.edu (Masatsugu Suzuki).

have shown that the boundary between the vortex liquid phase and the vortex glass phase corresponds to the de Almeida-Thouless (AT) [5] line for the spin glass behavior. Since then there have been a number of experimental works on the vortex glass phase in quasi 2D superconductors. Experimentally it has been confirmed that the H - T diagram consists of the vortex glass, vortex lattice (Abrikosov lattice), and vortex liquid phases. The boundary between the vortex lattice phase and the vortex liquid phase (the line H_{al}) is of the first order, while the boundary between the vortex lattice phase and the vortex glass phase (the line H_{ag}) and the boundary between the vortex glass phase and the vortex liquid phase (the line H_{gl}) are of the second order. These boundaries merge into a multicritical point at $T = T^*$ and $H = H^*$.

Sn-metal graphite (MG) constitutes a novel class of materials having unique layered structures. This system can be prepared by reduction of an acceptor-type SnCl_2 graphite intercalation compound (GIC) as a precursor material. Ideally, the staging structure of Sn-MG would be the same as that of SnCl_2 GIC. Sn layer is sandwiched between adjacent graphene sheets. These sandwiched structures are periodically stacked along the c axis perpendicular to the basal plane of graphene sheets. Sn-MG undergoes a superconducting transition at a critical temperature T_c ($= 3.75$ K), which is close to that of bulk Sn [6]. The superconductivity occurs mainly in Sn metal layers, forming a quasi 2D superconductor (type-II).

In this paper we report results on the magnetic properties of Sn-MG from measurements of DC and AC magnetic susceptibility. Three methods are used to determine the H - T diagram: (i) the T dependence of the magnetization (M) in various states such as the FC (field-cooled) state, ZFC (zero-field cooled) state, IR (isothermal remnant) state, and TR (thermoremanent) state, (ii) the T , H , h , and f dependence of the dispersion (Θ'_1/h or χ') and absorption (Θ''_1/h or χ'') of the AC magnetic susceptibility, where h and f are the amplitude and frequency of the AC magnetic field, respectively, and (iii) the H dependence of M . We find that there are four lines (H_{ag} , H_{gl} , $H_{gl'}$ and H_{al}) in the H - T phase diagram, separating vortex liquid, vortex glass, and vortex lattice phase. These lines merge at the multicritical point located at $T^* = 3.4$ K and $H^* = 40$ Oe. The lines H_{gl} and $H_{gl'}$ are irreversibility lines, intersecting at a critical point at $T_0' = 2.5$ K and $H_0' = 160$ Oe. The line H_{gl} has an AT-power law form,[5] while the line $H_{gl'}$ has a Gabay-Thouless (GT)-power law form [7]. The nature of possible slow dynamics and nonlinearity in the vortex glass phase is examined from the measurement of Θ'_1/h and Θ''_1/h as a function of ω , h , T , and H .

2 Experimental procedure

The method of sample preparation in Sn-MG is similar to that in other MG's previously reported [8,9,10,11]. SnCl_2 graphite intercalation compound (GIC) samples as a precursor material, were prepared by heating a mixture of natural graphite flakes (grade: RFL 99.9 S) from Kropfmühl, Germany and an excess amount of SnCl_2 . The reaction was continued for three days at 400 °C in an ampoule filled with chlorine gas. The synthesis of Sn-MG was made by the reduction of SnCl_2 GIC. SnCl_2 GIC samples were kept for two days in a solution of lithium diphenylide in tetrahydrofuran (THF) at room temperature. Then the samples were filtered, rinsed by THF, and dried in air. The structure of Sn-MG thus obtained was examined by (00L) x-ray diffraction, and bright field images and selected-area electron diffraction (SAED) (Hitachi H-800 transmission electron microscope) operated at 200 kV. No pristine SnCl_2 and its hydrolisation products were left in the Sn layers. The details of sample preparation and characterization in Sn-MG will be reported elsewhere.

The Sn-MG sample consists of many small flakes. Each flake has a well-defined c axis. The sample in the present work is regarded as a powdered sample with the c axis randomly distributed in all directions, since these flakes are randomly piled inside the sample capsule. The measurements of DC and AC magnetic susceptibility were carried out using a SQUID magnetometer (Quantum Design MPMS XL-5). Before setting up a sample at 298 K, a remnant magnetic field was reduced to less than 3 mOe using an ultra-low field capability option. For convenience, hereafter this remnant field is noted as the state $H = 0$. (i) *ZFC and FC magnetic susceptibility*: The sample was cooled from 298 to 1.9 K at $H = 0$. After H was applied at 1.9 K, the zero-field cooled magnetization (M_{ZFC}) was measured with increasing T from 1.9 to 6 K. The sample was kept at 20 K for 20 minutes in the presence of H . Then the field cooled magnetization (M_{FC}) was measured with decreasing T from 6 to 1.9 K. (ii) *M-H loop*: The sample was cooled from 298 K to T at $H = 0$. The measurement was carried out with varying H from 0 to 3 kOe at T , from $H = 3$ to -3 kOe, and from $H = -3$ to 3 kOe. (iii) *M_{ZFC} vs H* : The sample was cooled from 298 K to T at $H = 0$. The ZFC magnetization M_{ZFC} at T was measured with increasing H from 0 to 250 Oe. (iv) *AC magnetic susceptibility*. The dispersion (Θ'_1/h) and the absorption (Θ''_1/h) was determined from the in-phase and out-of phase first harmonic (ω) component in the AC magnetization measurement [12]. The dispersion (Θ'_1/h) and the absorption (Θ''_1/h) were described by $\Theta'_1/h = \chi' + 3\chi'_3 h^2/4 + 5\chi'_5 h^4/8 + \dots$ and $\Theta''_1/h = \chi'' + 3\chi''_3 h^2/4 + 5\chi''_5 h^4/8 + \dots$, where χ'_{2n+1} and χ''_{2n+1} ($n = 1, 2, \dots$) are the real and imaginary parts of high-order nonlinear magnetic susceptibility, respectively. In the limit of $h = 0$, Θ'_1/h and Θ''_1/h coincide with the linear susceptibility χ' and χ'' , respectively. Before the measurement, the sample was cooled from 298 to 1.9 K at $H = 0$. (i) The T dependence of Θ'_1/h and Θ''_1/h

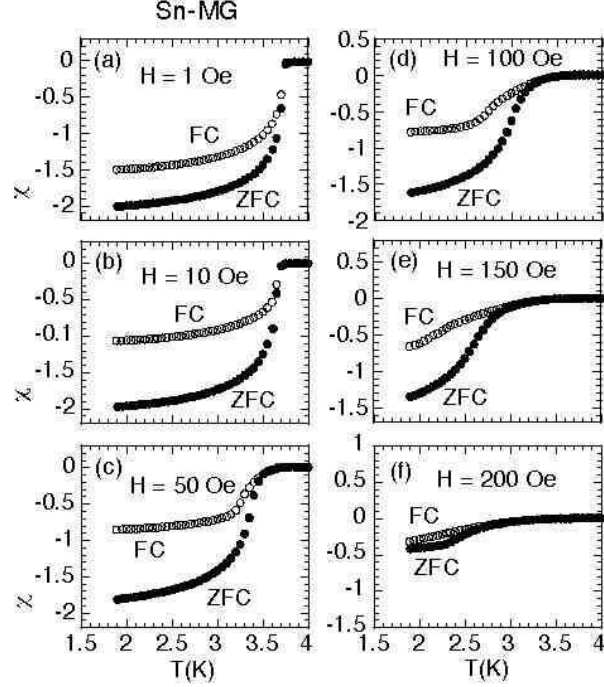


Fig. 1. (a) - (f) T dependence of χ_{FC} and χ_{ZFC} at low H ($1 \leq H \leq 200$ Oe) for Sn-MG.

was measured with increasing T from 1.9 to 6 K in the presence of H . After the measurement, the sample was cooled from 6 to 1.9 K in the presence of the same H . Then the measurement was repeated at different H . (ii) The h dependence was carried out at fixed T by changing h ($0.01 \leq h \leq 4$ Oe) at $f = 1$ Hz. (iii) The f dependence was carried out at fixed T in the presence of H by changing f ($0.1 \leq f \leq 1000$ Hz).

3 Result

3.1 χ_{FC} and χ_{ZFC}

Figure 1 shows the T dependence of χ_{FC} and χ_{ZFC} at low H . The susceptibility χ_{ZFC} deviates from χ_{FC} below a characteristic temperature for $1 \leq H \leq 200$ Oe, suggesting the irreversibility line in the H - T plane which separates the reversible region from the irreversible region. Figure 2 shows the T dependence of χ_{FC} and χ_{ZFC} for $1 \leq H \leq 3$ kOe. For $H \geq 300$ Oe there is no noticeable difference between χ_{FC} and χ_{ZFC} at any T . The susceptibility ($\chi_{ZFC} = \chi_{FC}$) exhibits a very broad peak, which shifts to the low- T side as H increases. In the inset of Fig. 2(a) we plot these peak temperatures as a function of H . The value of H ($= H_p$) for the peak is much larger than that of an upper critical field H_{c2} (whose definition will be given in Sec. 4.1) at the same T , and it

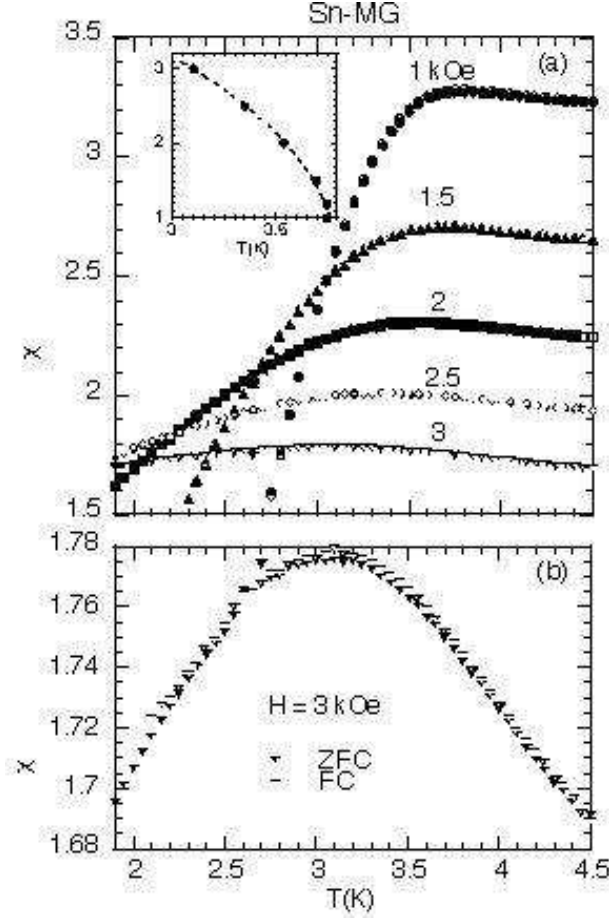


Fig. 2. T dependence of χ_{FC} and χ_{ZFC} at high H ($1 \leq H \leq 3$ kOe) for Sn-MG. The inset shows the plot of the peak temperature of χ_{FC} vs T as a function of H . The dotted line is a least-squares fitting curve. See the text for detail. (b) T dependence of χ_{FC} and χ_{ZFC} at $H = 3$ kOe, which is a blow-up of Fig. 2(a).

tends to zero around T_c . This result suggests that an antiferromagnetic (AF) short-range order survives at high H where the superconductivity disappears. The origin may be due to the possible antiferromagnetism of nanographites in Sn-MG (see Sec. 4.3).

Figure 3 shows the T dependence of the difference δ ($= \chi_{FC} - \chi_{ZFC}$) at various H . The difference δ for $H < H^*$ ($H^* \approx 40$ Oe) decreases with increasing T and reduces to zero at a characteristic temperature. In contrast, the difference δ for $H^* < H < 150$ Oe decreases in two steps with increasing T , showing a local minimum and a local maximum. The difference δ shows a small peak at 2.25 K for $H = 200$ Oe and is almost equal to zero for any T for $H = 250$ Oe.

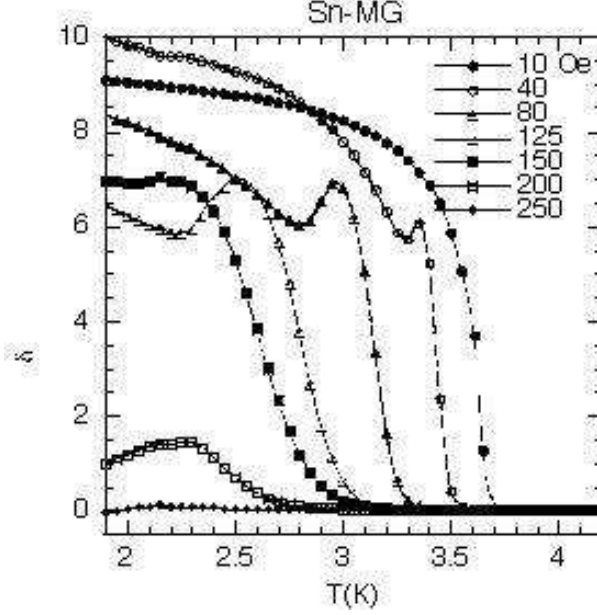


Fig. 3. T dependence of the difference δ ($= \chi_{FC} - \chi_{ZFC}$) at low H for Sn-MG. The solid lines are guides to the eyes.

3.2 M_{IR} and M_{TR}

In a mixed state of conventional type-II superconductors that have well-defined lower critical field H_{c1} and upper critical field H_{c2} ($H_{c1} < H < H_{c2}$), the thermodynamically most stable state involves filling the system with fluxoids, exhibiting only a partial Meissner effect with the magnetic induction $B = H + 4\pi M > 0$. Even a small degree of inhomogeneity is sufficient to pin some fluxoids at local free energy minima, so that some fluxoids remain trapped in place where H is removed. In Sn-MG the values of M and B are strongly dependent on the magnetic states such as the ZFC, FC, IR (isothermal remnant), and TR (thermoremnanant) states. Experimentally, the values of M and B for these states are obtained as follows. First the sample was cooled from 298 to 1.9 K at $H = 0$. Then H was applied. The measurements of M_{ZFC} and M_{IR} were done with increasing T from 1.9 to 4 K. At each T , M_{ZFC} was measured at H and then M_{IR} was measured 100 sec later after the field was changed from H to 0 Oe. Second, the sample was annealed at 20 K for 1200 sec at H . The measurements of M_{FC} and M_{TR} were done with decreasing T from 4 to 1.9 K. At each T , M_{FC} was measured at $H = 100$ Oe and then M_{TR} was measured 100 sec later after the field was changed from H to 0 Oe. The values of M and B for each state thus obtained are described by $B_{ZFC} = H + 4\pi M_{ZFC}$, $B_{IR} = 4\pi M_{IR}$, $B_{FC} = H + 4\pi M_{FC}$, and $B_{TR} = 4\pi M_{TR}$. Here B_{FC} and B_{ZFC} are the magnetic inductions in the FC and ZFC states with H , while B_{IR} and B_{TR} are the magnetic inductions in the IR and TR states with $H = 0$, respectively. These magnetic inductions result from the flux trapping at pinning centers. Figure 4(a) shows the T dependence of M_{ZFC} and

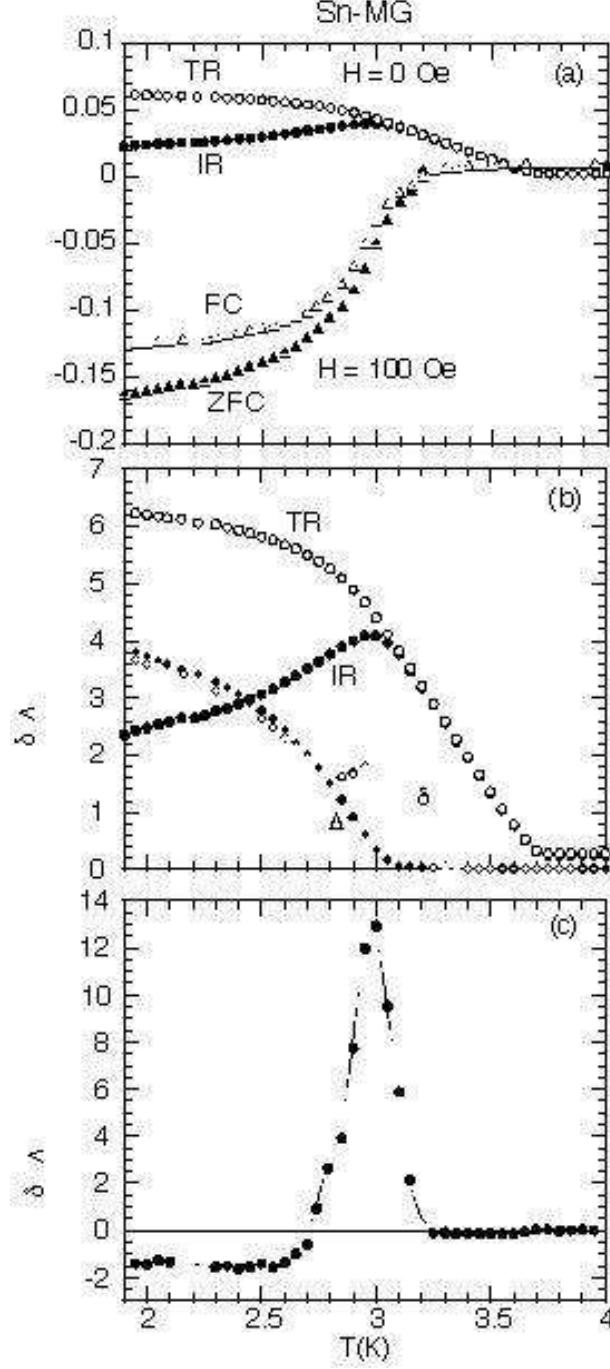


Fig. 4. (a) T dependence of M_{ZFC} , M_{IR} , M_{FC} , and M_{TR} for Sn-MG. The definition of these magnetizations and the method of the measurement are described in the text. $H = 100$ Oe. (b) T dependence of δ ($= M_{FC} - M_{ZFC}$), Δ ($= M_{TR} - M_{IR}$), M_{IR} , and M_{TR} . (c) T dependence of $(\delta - \Delta)$. The solid line is guide to the eyes.

M_{FC} at $H = 100$ Oe ($> H^*$), and M_{IR} and M_{TR} at $H = 0$. The T dependence of M_{IR} and M_{TR} is different from B_{IR} and B_{TR} by only a factor of 4π . The T dependence of M_{IR} and M_{TR} is similar to that of typical spin glass systems such as 3D Ising spin glass $\text{Fe}_c\text{Mn}_{1-c}\text{TiO}_3$ [13], where the competition between

the nearest neighbor antiferromagnetic and ferromagnetic interactions leads to the spin frustration effect. The magnetization M_{IR} exhibits a broad peak around 3.0 K, while M_{TR} decreases with increasing T . Both M_{IR} and M_{TR} reduce to zero at T_c , implying the appearance of both B_{IR} and B_{TR} below T_c . The deviation of M_{IR} from M_{TR} occurs below 3.1 K, showing the irreversible effect of magnetization. Note that the point at $T = 2.94$ K and $H = 100$ Oe is located on the line H_{gl} in the H - T diagram (see Sec. 4.1). Figure 4(b) shows the T dependence of Δ [$=M_{TR} - M_{IR} = (B_{TR} - B_{IR})/4\pi$] and δ [$=M_{FC} - M_{ZFC} = (B_{FC} - B_{ZFC})/4\pi$], as well as M_{IR} and M_{TR} . Figure 4(c) shows the T dependence of $(\delta - \Delta)$. The difference $(\delta - \Delta)$ is equal to zero at T above 3.25 K and exhibits a peak at 3.0 K where M_{IR} has a peak. It becomes negative below 2.7 K. The temperature region between 3.0 and 2.4 - 2.7 K corresponds to the vortex glass phase for $H = 100$ Oe.

Figures 5(a) - (c) show the T dependence of M_{FC} , M_{ZFC} , M_{IR} , M_{TR} , δ , Δ , and $\delta - \Delta$ for $H = 30$ Oe. The magnetization M_{IR} appears below T_c , exhibiting a peak at 3.5 K. Note that a point at $T = 3.5$ K and $H = 30$ Oe is located on the line H_{al} in the H - T diagram (see Sec. 4.1). The deviation of M_{IR} from M_{TR} occurs at T below 3.6 K, while the deviation of M_{ZFC} from M_{FC} occurs below 3.55 K. The difference $(\delta - \Delta)$ exhibits a very sharp peak at 3.5 K, being equal to zero above 3.6 K and below 3.4 K.

3.3 M vs H

Figure 6 shows the hysteresis loop of the magnetization M at $T = 1.9$ and 5 K. The M - H curve at 1.9 K shows a typical superconducting behavior with a negative local minimum around $H = 160$ Oe, corresponding to the phase boundary (the line H_{ag}) between the vortex lattice and vortex glass phase (see Sec. 4.1). The M - H curve is not reversible, partly because some fluxoids remain trapped at pinning centers when H is removed. The M - H curve at 5 K is not perfectly proportional to H . The susceptibility M/H is estimated to be 3.45×10^{-6} emu/g at $H = 1$ kOe, which is in contrast to the negative diamagnetic susceptibility of pristine graphite: $\chi = -30 \times 10^{-6}$ emu/g for H along the c axis and -5.5×10^{-7} emu/g along the basal plane (so-called c plane) perpendicular to the c axis below 100 K [14].

Figures 7(a) and (b) show typical data of M_{ZFC} vs H at various T . The sample was cooled from 298 K to T (< 4 K) at $H = 0$. The magnetization M_{ZFC} at T was measured with increasing H ($0 < H < 250$ Oe). The magnetization M_{ZFC} exhibits a single local minimum at a characteristic field for $T < T_c$. Similar behavior has been reported in $\text{YBa}_2\text{Cu}_3\text{O}_{6.92}$ by Shibata et al. [15]. It seems that a discontinuous change in M_{ZFC} is observed just above the characteristic field for $T^* < T < T_c$, where $T^* = 3.4$ K and $T_c = 3.75$ K. The field of the

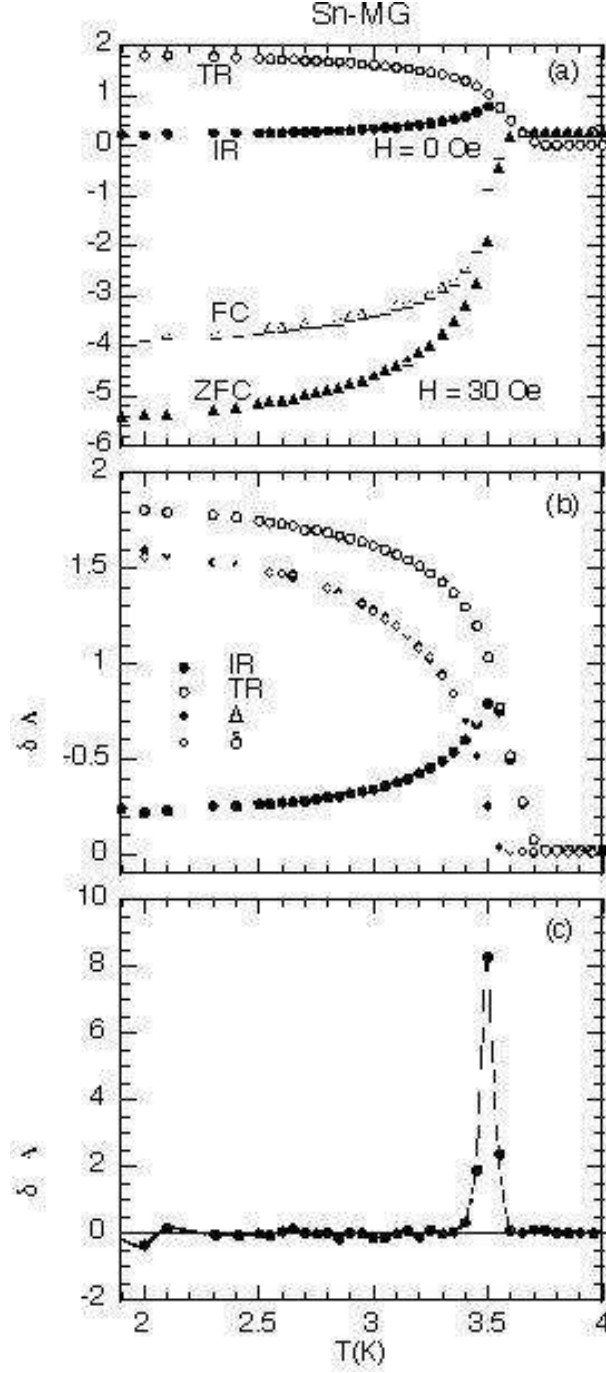


Fig. 5. (a) T dependence of M_{ZFC} , M_{IR} , M_{FC} , and M_{TR} for Sn-MG. $H = 30$ Oe. (b) T dependence of δ ($= M_{FC} - M_{ZFC}$), Δ ($= M_{TR} - M_{IR}$), M_{IR} , and M_{TR} . (c) T dependence of $(\delta - \Delta)$. The solid line is guide to the eyes.

local-minimum for M_{ZFC} vs H , which is plotted as a function of T , forms the line H_{ol} of the first order transition in the H - T plane (see Sec. 4.1). The jump height ΔM_{ZFC} , which is defined as the difference between the value of M_{ZFC} at which M_{ZFC} starts to be proportional to H and the local-minimum value of M_{ZFC} vs H , rapidly decreases with increasing T and reduces to zero at T_c . The

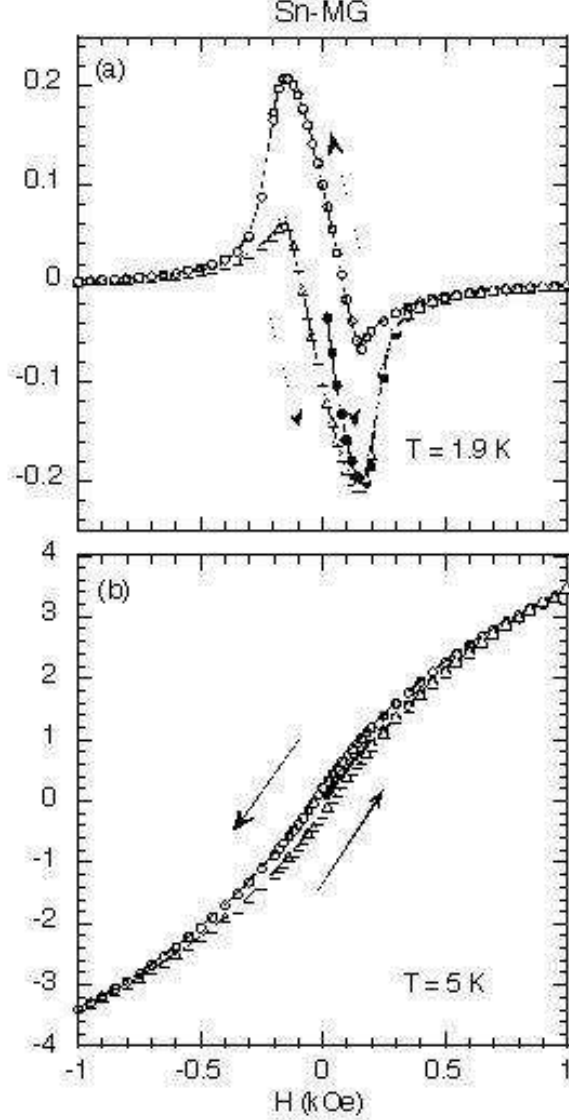


Fig. 6. Magnetization loop (M vs H) for Sn-MG. (a) $T = 1.9$ K and (b) 5 K. The method of the measurement is described in the text. The solid lines are guides to the eyes.

jump height ΔM_{ZFC} may be described by $\Delta M_{ZFC} = M_l - M_a$ [16], where M_l and M_a denote the magnetization in the vortex liquid and the vortex lattice phase, respectively. The positive value of ΔM_{ZFC} implies that the vortex density in the vortex liquid phase is higher than that in the vortex lattice phase. The magnetization M_{ZFC} at $T = 3.7$ and 3.8 K is almost proportional to H with a positive slope. The derivative dM_{ZFC}/dH at 3.7 and 3.8 K shows a broad peak around $H = 100$ Oe, suggesting the existence of AF short-range order. The origin of the AF short-range order is due to nanographites in Sn-MG (see Sec. 4.3). Note that a discontinuous jump of M_{ZFC} in the vicinity of $M_{ZFC} = 0$ is an artifact due to the SQUID measurement. Such a jump in the magnetization is frequently observed when the magnetization changes its

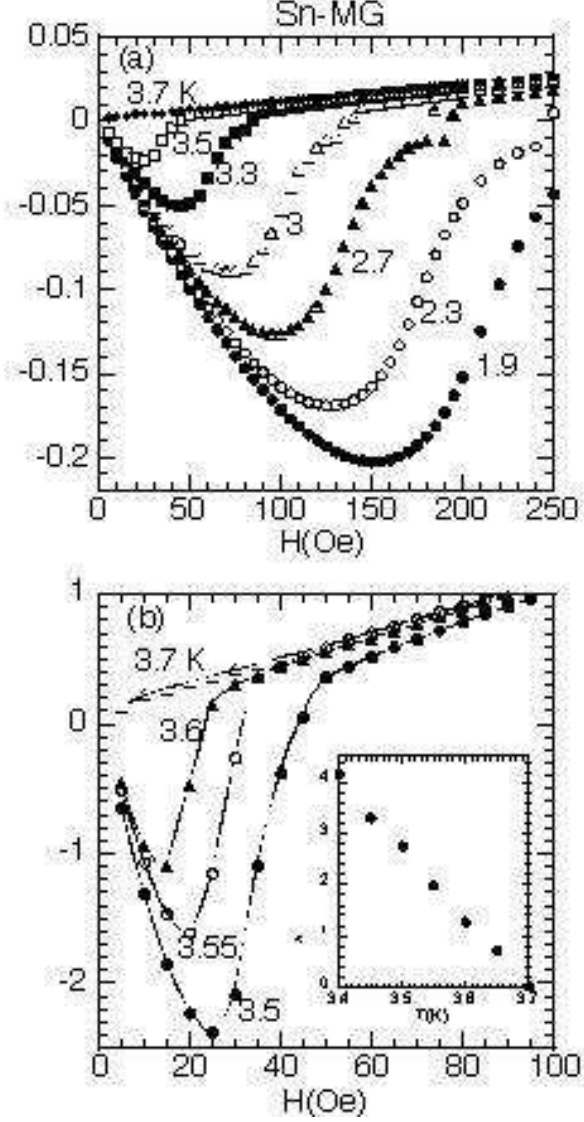


Fig. 7. (a) and (b) M_{ZFC} vs H at various T . The solid lines are guides to the eyes. The inset of Fig. 7(b) shows the jump in magnetization ΔM_{ZFC} (which is defined in the text) as a function of T .

sign.

The lower critical field $H_{c1}(T)$ is defined as a field at which the curve of M vs H starts to deviate from the linear portion due to the penetration of the magnetic flux into the system: $H_{c1}(T = 1.9 \text{ K}) = 20 \pm 5 \text{ Oe}$.

3.4 χ' and χ''

Figure 8 shows the T dependence of the dispersion χ' at various H , respectively, where $f = 1 \text{ Hz}$ and $h = 0.1 \text{ Oe}$. The AC response to such a small

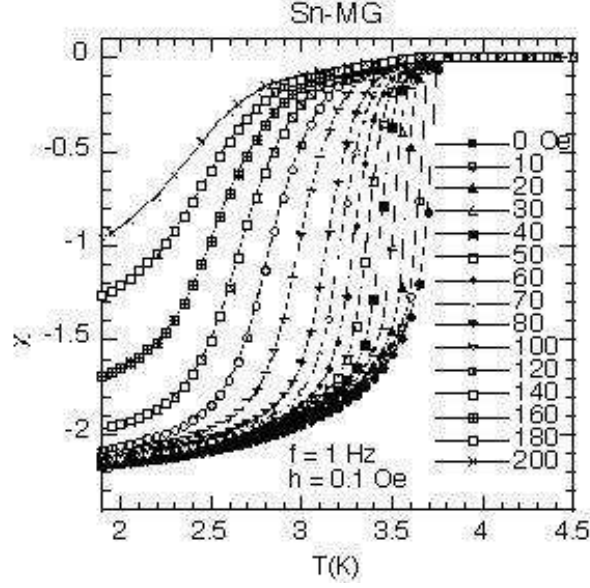


Fig. 8. T dependence of χ' at various H for Sn-MG. $h = 0.1$ Oe. $f = 1$ Hz. The solid lines are guides to the eyes.

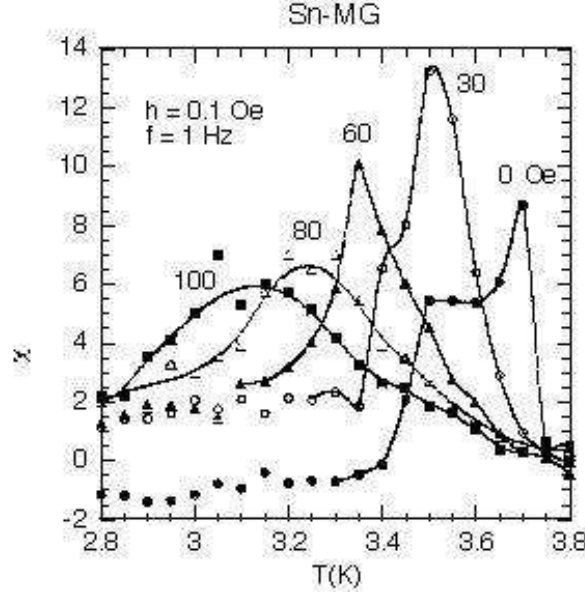


Fig. 9. T dependence of χ'' at various H for Sn-MG. $h = 0.1$ Oe. $f = 1$ Hz. The solid lines are guides to the eyes.

h is found to be linear in the whole range of temperatures and fields. The derivative $d\chi'/dT$ shows a sharp peak at T_c at $H = 0$, shifting to the low- T side with increasing H . The peak temperature for $d\chi'/dT$ vs T plotted as a function of H in the H - T diagram forms the line H_{gl} for $H > H^*$ and the line H_{al} for $H < H^*$ (see Sec. 4.1).

Figure 9 shows the T dependence of the absorption χ'' at various H , where $f = 1$ Hz and $h = 0.1$ Oe. The absorption χ'' at $H = 0$ seems to have two

peaks at T_c and 3.5 K. The peak at T_c at $H = 0$ shifts to the low- T side with increasing H . In contrast, the peak at 3.5 K at $H = 0$ remains unshifted, becoming a shoulder even at 10 Oe, and tends to disappear above $H = 30$ Oe. Note that the peak temperature of the main peak for χ'' vs T is slightly higher than that for $d\chi'/dT$ vs T at the same H . The peak temperature for χ'' vs T is plotted as a function of H in the H - T diagram, forming the line H_{al} for $H < H^*$ and a new line $H_{gl'}$ for $H > H^*$ which deviates from the line H_{gl} for $H^* < H < 150$ Oe (see Sec. 4.1). The main peak of χ'' vs T is sharp for $H < H^*$ but becomes much broad for $H > H^*$.

3.5 Θ'_1/h and Θ''_1/h

The AC response (Θ'_1/h and Θ''_1/h) for sufficiently large amplitude of the AC magnetic field becomes nonlinear below T_c . In fact, as it will be shown later, the T dependence of Θ''_1/h is strongly dependent on h for $h \geq 0.2$ Oe. This is in contrast to the case of $h = 0.1$ Oe, where the linearity is valid: $\Theta'_1/h = \chi'$ and $\Theta''_1/h = \chi''$. Here a large amplitude of the AC magnetic field ($h = 2$ Oe) was used to examine the effect of nonlinearity on the vortex glass phase. Figure 10 shows the T dependence of Θ'_1/h and Θ''_1/h for Sn-MG at various f ($0.1 \leq f \leq 1000$ Hz) in the presence of H ($= 100$ Oe), where $h = 2$ Oe. The T dependence of Θ'_1/h is almost independent of f , while the T dependence of Θ''_1/h is strongly dependent on f . The shape of Θ''_1/h vs T does not change with f but the basement of Θ''_1/h proportionally increases with increasing f for $0.1 \leq f \leq 1000$ Hz at any T below T_c . As shown in Fig. 10(b) there are two broad peaks at 2.90 and 3.15 K for Θ''_1/h with $h = 2$ Oe. These peaks do not shift with f for $0.1 \leq f \leq 1000$ Hz within the experimental error in T (typically $\Delta T_c = 0.01$ K). No relaxation time effect is observed, suggesting $\omega\tau \ll 1$, where τ is the relaxation time of the vortex system and ω ($=2\pi f$) is the measured angular frequency. This is very different from the case of typical spin-glass systems where $\omega\tau \approx 1$ and the peak of Θ''_1/h shifts to the high T side with increasing f [17]. We show that the T and f dependence of Θ'_1/h and Θ''_1/h are explained in terms of the screening behavior arising from skin size effects. The absorption peak occurs when the electromagnetic penetration depth δ_s becomes comparable to the sample size L (see Sec. 4.2). The peak at 3.15 K coincides with that of χ'' at $h = 0.1$ Oe and $f = 1$ Hz (see Fig. 9). The point at $H = 100$ Oe and $T = 3.15$ K is located on the line $H_{gl'}$. On the other hand, the peak at 2.9 K is newly observed for $h = 2$ Oe. The point at $H = 100$ Oe and $T = 2.9$ K is located on the line H_{gl} . Note that the data of $d\chi'/dT$ vs T shows a peak at 2.94 K and $d\delta/dT$ has a local minimum at 3.0 K. In this sense, the line H_{gl} is the irreversibility line.

Figure 11 shows the T dependence of Θ''_1/h for Sn-MG at various f ($0.1 \leq f \leq 1000$ Hz) in the presence of H ($= 70$ Oe), where $h = 2$ Oe. There are

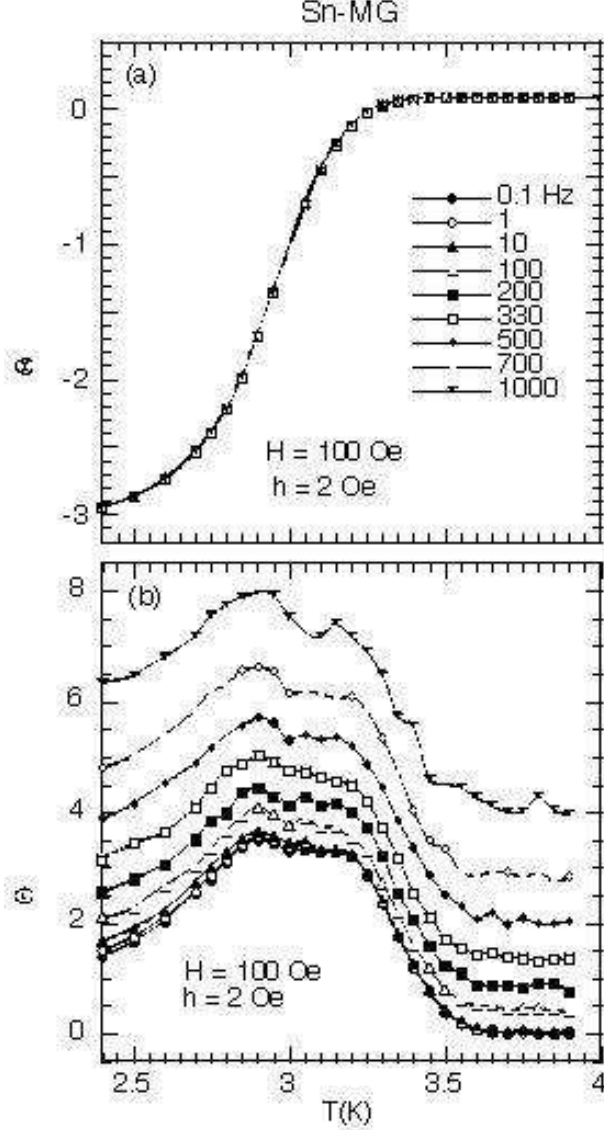


Fig. 10. T dependence of (a) the dispersion Θ'_1/h and (b) the absorption Θ''_1/h at various f ($0.1 \leq f \leq 1000$ Hz) for Sn-MG. $H = 100$ Oe. Because of the nonlinearity, Θ'_1/h at $h = 2$ Oe is not equal to χ'' at $h = 0.1$ Oe (see Fig. 12(b) for the nonlinearity at $H = 0$). The solid lines are guides to the eyes.

two peaks at 3.1 - 3.15 K and 3.3 - 3.4 K. It seems that these peaks do not shift with f . This result suggests no occurrence of the relaxation time effect for $0.1 \leq f \leq 1000$ Hz. The peak at 3.3 - 3.4 K coincides with that at 3.34 K of χ'' at $h = 0.1$ Oe and $f = 1$ Hz (the data at $H = 70$ Oe are not shown in Fig. 9). The point at $H = 70$ Oe and $T = 3.3 - 3.4$ K is located on the line $H_{gl'}$. On the other hand, the peak at 3.1 - 3.15 K is newly observed for $h = 2$ Oe. The point at $H = 70$ Oe and $T = 3.1 - 3.15$ K is located on the line H_{gl} . Figure 12 shows the h dependence of (a) Θ'_1/h and (b) Θ''_1/h for Sn-MG at various T in the absence of H , where $0.01 \leq h \leq 4$ Oe. Both Θ'_1/h and Θ''_1/h are not independent of h for $h > 0.2$ Oe, indicating the nonlinearity of the AC

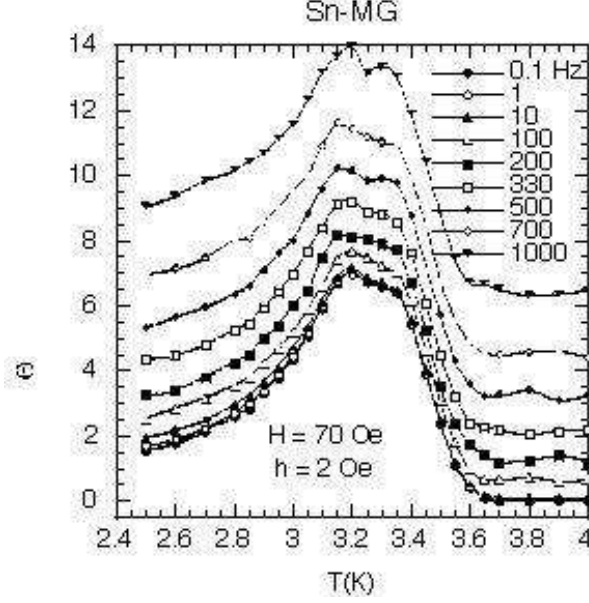


Fig. 11. T dependence of Θ'_1/h at various f ($0.1 \leq f \leq 1000$ Hz) for Sn-MG. $H = 75$ Oe. $h = 2$ Oe. The solid lines are guides to the eyes.

response. The dispersion Θ'_1/h linearly changes with h below T_c , but is almost independent of h at 3.8 K just above T_c .

4 Discussion

4.1 H - T phase diagram

Our results obtained above are summarized in the H - T diagram. In Figs. 13(a) and (b), we make a plot of the peak temperatures of $d\chi'/dT$ vs T and χ'' vs T , and the local-minimum temperatures of $d\delta/dT$ vs T as a function of H , and the local-minimum fields of M_{ZFC} vs H as a function of T . We find that these data lie on the phase boundaries denoted by the lines H_{ag} , H_{gl} , $H_{gl'}$, and H_{al} , which separate the vortex lattice, vortex glass, and vortex liquid phase. These lines merge at the multicritical point at $T^* = 3.4$ K and $H^* = 40$ Oe. The lines H_{ag} , H_{gl} , and $H_{gl'}$ are of the second order, while the line H_{al} is of the first order. The line H_{c2} is a crossover line separating the normal phase at higher temperatures from the vortex liquid phase. (i) On the line H_{gl} , the data of $d\chi'/dT$ vs T have a peak at fixed H , the data of $d\delta/dT$ vs T have a local minimum, and the data of χ'' vs T have a peak for $H \geq 160$ Oe. (ii) On the line $H_{gl'}$, the data of χ'' vs T have a peak at fixed H . (iii) On the line H_{ag} , the data of $d\delta/dT$ vs T have a local minimum at fixed H and the data of M_{ZFC} vs H have a local minimum at fixed T . (iv) On the line H_{al} , the data of $d\chi'/dT$ vs T and χ'' vs T have a peak at fixed H , the data of $d\delta/dT$ vs T

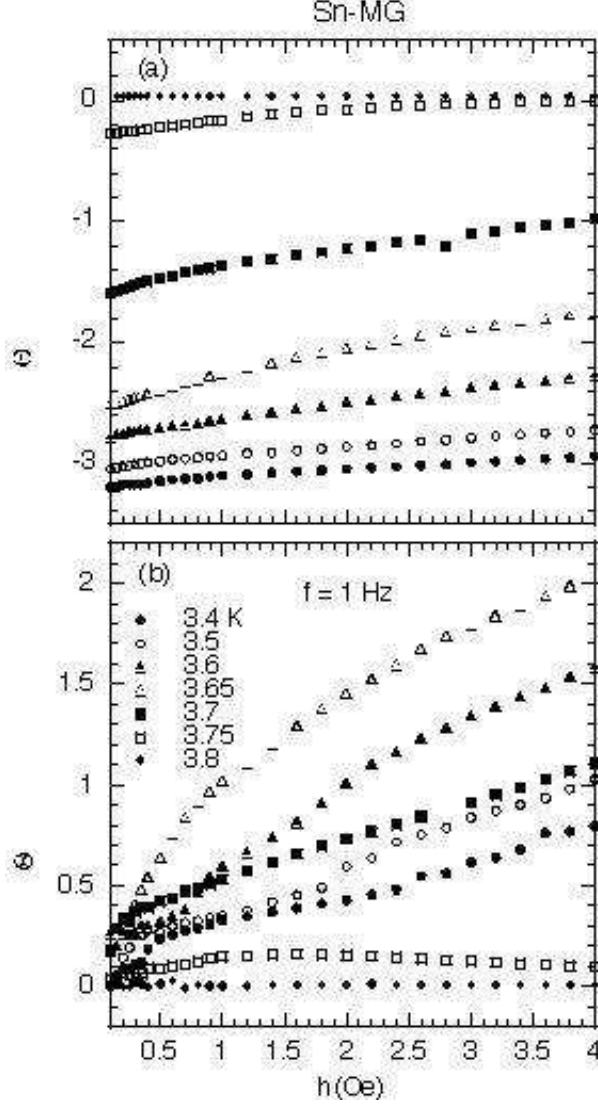


Fig. 12. h dependence of (a) Θ'_1/h and (b) Θ''_1/h at various T for Sn-MG. $f = 1$ Hz. $H = 0$.

have a local minimum at fixed H , and the data of M_{ZFC} vs H have a local minimum at fixed T . (v) On the line H_{c2} , the data of χ_{ZFC} vs T come to take a saturated value $\chi_{ZFC}^{(s)}$ at fixed H . The susceptibility $\chi_{ZFC}^{(s)}$ is positive and weakly dependent on H . It takes 1.8×10^{-7} emu/g at $H = 10$ Oe, increasing with increasing H , and reaches a peak ($= 4.63 \times 10^{-6}$ emu/g) at $H = 200$ Oe. In turn it decreases with further increasing H , and reaches 3.75×10^{-6} emu/g at $H = 1$ kOe (see Fig. 3(a)).

Using an empirical relation given by Werhammer et al. [18], $H_{c2}(T = 0 \text{ K}) = -0.69T_c(dH_{c2}/dT)_{T_c}$, the value of H_{c2} at $T = 0$ K can be estimated as $H_{c2}(0) = 1850 \pm 20$ Oe, where we use $T_c = 3.75$ K and a slope $(dH_{c2}/dT)_{T_c} = -714.4 \pm 6.8$ (Oe/K) obtained from the linear relation in H_{c2} vs T in the vicinity of $T = T_c$ and $H_{c2} = 0$. The coherence length $\xi(0)$ can be estimated

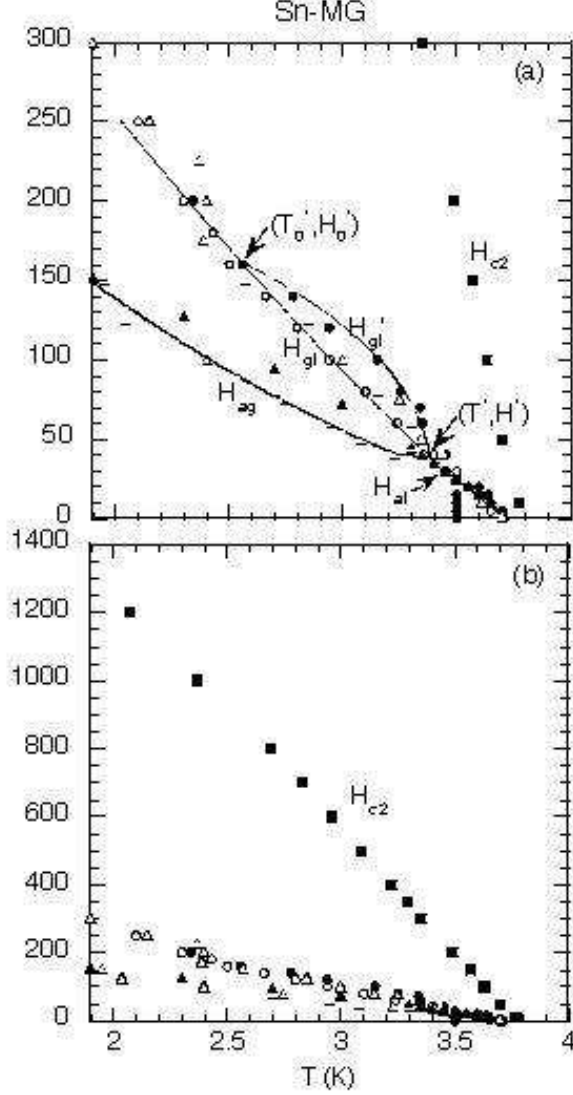


Fig. 13. (a) and (b) H - T diagram for Sn-MG. The peak temperatures of $d\chi'/dT$ vs T (O), χ'' vs T (●), and the local-minimum temperatures of $d\delta/dT$ vs T (Δ) are plotted as a function of H . The local-minimum fields of M_{ZFC} vs H (▲) are plotted as a function of T . The vortex lattice (Abrikosov lattice), vortex liquid, and vortex glass phases are separated by the lines H_{al} , H_{ag} , H_{gl} , and $H_{gl'}$. These lines merge at the multicritical point located at $(T^* \approx 3.4 \text{ K}, H^* \approx 40 \text{ Oe})$. The line H_{c2} is a crossover line denoted by closed squares (■). The lower critical line H_{c1} is not shown in this figure. $H_{c2}(T = 0\text{K}) \approx 1.85 \text{ kOe}$. The solid lines for the lines H_{gl} , $H_{gl'}$, H_{ag} , and H_{al} denote the least-squares fitting curves of the data for H_i vs T to Eq.(1) with $i = gl, gl', ag$, and al , respectively. The corresponding parameters are given in the text.

as $420 \pm 20 \text{ \AA}$ using a relation $H_{c2}(0) = \Phi_0 / (2\pi\xi(0)^2)$, where $\Phi_0 (= 2.0678 \times 10^{-7} \text{ Gauss cm}^2)$ is a fluxoid. Note that our value of $H_{c2}(0)$ for Sn-MG is on the same order as that of Sn films grown on an InSb (110) surface [19]. The value of $H_{c2}(0)$ strongly depends on the thickness t of the Sn films: $H_{c2}(0) = 3160$

Oe for $t = 420\text{\AA}$ and 2540 Oe for $t = 2540\text{\AA}$ for H parallel to the Sn film.

Here we assume that the T dependence of the line H_i ($i = gl, gl', ag$, and al) may be described by a power law form given by

$$H = H_i^*(1 - T/T_i^*)^{\alpha(i)}, \quad (1)$$

where $\alpha(i)$ is an exponent, and H_i^* and T_i^* are characteristic field and temperature, respectively. The least squares fit of the data of H vs T ($40 \leq H \leq 250$ Oe) obtained from the peak temperature of $d\chi'/dT$ vs T at H , to Eq.(1) with $i = gl$ yields the parameters $\alpha(gl) = 1.43 \pm 0.05$, $T_{gl}^* = 3.90 \pm 0.08$ K, and $H_{gl}^* = 730 \pm 20$ Oe. The exponent $\alpha(gl)$ is close to that ($= 1.50$) predicted from the AT theory [5], suggesting that the line H_{gl} is the so-called irreversibility line separating a higher-temperature vortex liquid phase from a lower-temperature vortex glass phase. The least squares fit of the data of H vs T ($70 \leq H \leq 160$ Oe) obtained from the peak temperature of χ'' vs T at H , to Eq.(1) with $i = gl'$ yields the parameters $\alpha(gl') = 0.57 \pm 0.10$, $T_{gl'}^* = 3.57 \pm 0.09$ K, and $H_{gl'}^* = 330 \pm 10$ Oe. The exponent $\alpha(gl')$ is close to that ($= 0.50$) predicted from the Gabay-Thoules (GT) theory [7]. Such an occurrence of the AT-GT crossover has been reported in granular high T_c superconductors [20,21]. No GT-power law form has been observed in a single crystal of $\text{YBa}_2\text{Cu}_3\text{O}_7$ without granularity [20]. These results suggest that the AT-GT crossover behavior is indicative of the frustrated nature of the system due to disorder and granularity. This crossover is an analogy to the Ising-Heisenberg crossover behavior observed in Heisenberg-like spin glasses [22]. Such a crossover occurs when the magnetic field collapses the random local anisotropy field. The AT and GT lines in SG systems represent the longitudinal and transverse freezing, respectively.

Similarly, the least-squares fit of the data of H vs T ($40 \leq H \leq 150$ Oe) obtained from the peak temperature of $d\chi'/dT$ vs T at H , to Eq.(1) with $i = ag$ yields the parameters $\alpha(ag) = 2.06 \pm 0.05$, $T_{ag}^* = 4.77 \pm 0.80$ K, and $H_{ag}^* = 435 \pm 50$ Oe. Note that the lower critical field $H_{cl}(0)$ is much lower than H_{ag}^* . The least-squares fit of the data of H vs T ($0 \leq H \leq 40$ Oe) obtained from the peak temperature of $d\chi'/dT$ vs T at H , to Eq.(1) with $i = al$ yields the parameters $\alpha(al) = 1.02 \pm 0.03$, $T_{al}^* = 3.70 \pm 0.02$ K, and $H_{al}^* = 580 \pm 50$ Oe. The value of $\alpha(al)$ is in good agreement with the mean-field value ($= 1$) derived from the Ginzburg-Landau theory [23], where the correlation length varies with $(1 - T/T_{al}^*)^{-1/2}$.

The H - T diagram of Sn-MG is similar to that of a quasi-2D superconductors (type-II). The field for the multicritical point ($= H^*$) is described by the dimensional crossover field that separates the region of 2D thermal fluctuations (for $H > H^*$) and the 3D thermal fluctuations ($H < H^*$). In this sense, the H - T diagram may be universal for any quasi-2D superconductors when the H

axis and T axis are scaled by H/H^* and T/T_c , respectively. For $\text{YBa}_2\text{Cu}_3\text{O}_7$ with $T_c = 90$ K, the multicritical point is located at $T^* = 76$ K and $H^* = 90$ kOe [2]. The ratio T^*/T_c for $\text{YBa}_2\text{Cu}_3\text{O}_7$ is 0.84, which is almost equal to that ($= 0.91$) for Sn-MG with $T^* = 3.4$ K and $T_c = 3.75$ K.

4.2 Nature of the lines H_{gl} and $H_{gl'}$

Here we discuss the origin of the irreversibility lines $H_{gl'}$ and H_{gl} for $H^* < H < 160$ Oe. We find the following results on the T dependence of AC magnetic susceptibility at small AC field ($h = 0.1$ Oe) and large AC field ($h = 2$ Oe). (i) The linear absorption χ'' at $h = 0.1$ Oe exhibits a peak only on the line $H_{gl'}$. (ii) The nonlinear absorption Θ_1''/h exhibits a peak on the line $H_{gl'}$ and a peak on the line H_{gl} .

It is assumed that there is an irreversibility line $T_{gl}(H)$ (or the line $H_{gl}(T)$) in the H - T plane which separates an Ohmic region [$T > T_{gl}(H)$] from a non-Ohmic region [$T < T_{gl}(H)$]. Above $T_{gl}(H)$, a voltage V is proportional to current I , whereas below $T_{gl}(H)$, V shows an extremely nonlinear dependence where the linear resistivity is zero and the electric field E is described by $E \approx \exp(-A/J^\mu)$ [24]. Here A and μ are positive constants and J is the current density.

Why does the peak of the absorption for small AC field amplitude appear on only the line $H_{gl'}$ for $H > H^*$? Why does the peak of the absorption for large AC field amplitude appear on both the lines H_{gl} and $H_{gl'}$ for $H > H^*$? Similar problem was addressed first by Geshkenbein et al. [24] and later by Steel and Graybeal [25]. According to their skin size effect hypothesis, the peak of Θ_1''/h appears when the electromagnetic penetration depth $\delta_s = (c^2\rho/f)^{1/2}/2\pi$ is on the order of the system size L , or when ω coincides with the characteristic angular frequency ω_{peak} given by

$$\omega_{peak} = 0.8c^2\rho(T, H)/L^2, \quad (2)$$

where $\rho(T, H)$ is the electrical resistivity. Then Θ_1''/h is a function of only ω/ω_{peak} , and has a peak at $\omega = \omega_{peak}$. When δ_s becomes infinity, the field penetrates the system completely and Θ_1''/h tends to zero. In the opposite limiting case ($\delta_s \rightarrow 0$), the screening is complete and $\Theta_1''/h = 0$.

First we consider the peak temperature $T_{peak}(H)$ of Θ_1''/h at any h , where $T_{peak}(H) > T_{gl}(H)$. We assume that the response of the system is linear (Ohmic). The current density is of the order of $J_{peak} = ch/(4\pi L)$. The resistivity $\rho(T, H) = E(J_{peak})/J_{peak}$, which is independent of J_{peak} , decreases with decreasing T and tends to zero at $T_{gl}(H)$. The peak temperature $T_{peak}(H)$

can be determined from the matching condition ($\omega = \omega_{peak}$) given by Eq.(2): $T = T_{peak}^{(1)}$ for $f_1 = 0.1$ Hz and at $T = T_{peak}^{(2)}$ for $f_2 = 1$ kHz. Then we have a relation $\rho(T_{peak}^{(2)}, H)/\rho(T_{peak}^{(1)}, H) = 10^4$. Since there is no shift of $T_{peak}(H)$ in Θ_1''/h with f ($0.1 \leq f < 1000$ Hz) in the present work, it follows that the difference of peak temperatures defined by $\Delta T = T_{peak}^{(2)} - T_{peak}^{(1)}$ should be less than 0.01 K. Because of the sharp drop in resistivity with decreasing T , $T_{peak}(H)$ thus obtained is very close to but above $T_{gl}(H)$. The value of $T_{peak}(H)$ is independent of h because Eq.(2) is independent of h . The resistivity is finite at $T = T_{peak}(H)$: $\rho_{min} = \rho(T_{peak}, H) = 1.25\omega L^2/c^2$. In summary, Θ_1''/h vs T has a peak at $T_{peak}(H)$ just above $T_{gl}(H)$, which is independent of h .

Next we consider the peak temperature $T_{peak}(H)$ of Θ_1''/h at any h , where $T_{peak}(H) < T_{gl}(H)$. We assume that the response of the system is highly non-linear (non-Ohmic). The effective resistivity is defined by $\rho_{eff}(J_{peak}, T, H) = E(J_{peak})/J_{peak}$, where $J_{peak} = ch/(4\pi L)$. As a function of T , ρ_{eff} decreases with decreasing T and tends to zero at a temperature below $T_{gl}(H)$. As a function of J_{peak} , ρ_{eff} has a local minimum at $J_{peak} = (A\mu)^{1/\mu}$, and is equal to zero at both $J_{peak} = 0$ and $J_{peak} = \infty$. When J_{peak} is smaller than $(A\mu)^{1/\mu}$ [or $h < 4\pi L(A\mu)^{1/\mu}/c$], $\rho_{eff}(J_{peak})$ decreases with decreasing J_{peak} (or with decreasing h). The peak temperature $T_{peak}(H)$ can be estimated from Eq.(2) with $\rho(T, H) = \rho_{eff}(J_{peak})$: $\rho_{eff}(J_{peak}) = 1.25\omega L^2/c^2$ at $T = T_{peak}(H)$. The value of J_{peak} (or h) is uniquely determined because of the relation between J_{peak} and h . The peak temperature $T_{peak}(H)$, which is lower than $T_{gl}(H)$, increases with decreasing h and approaches the line $T_{gl}(H)$ from the low- T side. In summary, Θ_1''/h vs T has a peak at $T_{peak}(H)$ just below $T_{gl}(H)$ for sufficiently large h satisfying the above condition.

The lines H_{gl} and $H_{gl'}$ intersect at a critical point located at $T'_0 = 2.5$ K and $H'_0 = 160$ Oe. The line H_{gl} line for $H > H'_0$ no longer separates the irreversible region of the vortex glass phase from the reversible region of the vortex liquid phase. In this sense, the vortex glass phase may connect smoothly to the vortex liquid phase at the critical point at T'_0 and H'_0 [3]. As shown in Fig. 3, in fact the T dependence of δ at $H \geq 200$ Oe is rather different from that at 150 Oe. The difference δ at $H \geq 250$ Oe is almost equal to zero at any T , indicating the reversibility of magnetization on the line $H_{gl}(T)$.

The line $H_{gl}(T)$ may correspond to the AT line of spin glasses [5]. Then it is expected that the relaxation time of Sn-MG, τ , diverges as a power law form $\tau = \tau_0[T/T_{gl}(H) - 1]^{-x}$ [1], as T approaches the irreversibility line $T_{gl}(H)$ from the high- T side. Here τ_0 is a characteristic relaxation time and x is a dynamic critical exponent. Experimentally, no relaxation time effect is observed in the T and f dependence of Θ_1'/h and Θ_1''/h on the line $H_{gl}(T)$ (see Sec. 3.5). This result indicates that the condition $\omega\tau \ll 1$ is satisfied, in spite of crossing the line $H_{gl}(T)$. Thus the power law form is not the case of the present system. What is the origin of τ satisfying the condition $\omega\tau \ll 1$? The absorption of the

AC field is mainly governed by the hopping of the vortices over the barriers between different metastable states. The depinning time τ for such intervalley transition is obtained from a characteristic relaxation time τ_0 by an Arrhenius form $\tau \approx \tau_0 \exp(U_0/k_B T)$, where U_0 is the activation barrier energy between the different metastable states [24,25]. Then τ smoothly changes as T changes and $\omega\tau \ll 1$ on the line $H_{gl}(T)$.

In summary, it is concluded from the experimental results described above that the properties of the vortex glass phase in Sn-MG are characterized as follows, although most of them are not sufficiently understood at present. (i) The magnetization M_{ZFC} deviates from M_{FC} below $T_{gl}(H)$ for $H > H^*$. (ii) The magnetization M_{IR} deviates from M_{TR} below $T_{gl}(H)$. The T dependence of M_{IR} and M_{TR} is very similar to that of M_{ZFC} and M_{FC} in typical spin glass systems, respectively [17]. (iii) The difference $(\delta - \Delta)$ takes a positive large value for the vortex glass phase, while it is equal to zero for the vortex liquid phase and it takes a negative value in the vortex lattice phase. (iv) The relaxation time τ shows no behavior of divergence on the line $T_{gl}(H)$. (v) The non-Ohmic behavior is observed in the vortex glass phase, while the Ohmic behavior is observed in the vortex liquid phase.

4.3 Antiferromagnetic short-range order

There are several results supporting the existence of the AF short-range order. The first evidence is the T dependence of the peak field H_p as shown in the inset of Fig. 2. The field H_p is much higher than H_{c2} at the same T : $H_p \approx 3.2$ kOe and $H_{c2} \approx 490$ Oe at 3.0 K. The field H_p increases with decreasing T and may be described by a power law form given by $H_p = H_p^*(1 - T/T_p^*)^\beta$, where β is an exponent, and H_p^* and T_p^* are characteristic field and temperature, respectively. The least squares fit of the data of H_p vs T ($1 \leq H \leq 3$ kOe) to the power law form yields the parameters $\beta = 0.41 \pm 0.02$, $T_p^* = 3.82 \pm 0.02$ K, and $H_p^* = 5.95 \pm 0.05$ kOe. The exponent β is close to $\beta = 1/2$ for the molecular field theory. The temperature T_p^* is a little higher than T_c . The second evidence is the magnitude of the DC magnetic susceptibility: $\chi = 3.45 \times 10^{-6}$ emu/g at $H = 1$ kOe and $T = 5$ K. This value of χ is positive and is very different from that of pristine graphite which is diamagnetic (see Sec. 3.3) [14].

What is the origin of the AF short-range order? The existence of the AF short-range order has been observed in other MG's such as Bi-MG [26]. In these MG's the metal layers would generate internal stress inside the graphite lattice, leading to the break up of adjacent graphene sheets into nanographites. Fujita et al. [27] and Wakabayashi et al. [28] have theoretically suggested that the electronic structures of finite-size graphene sheets depend crucially on the shape of their edges (zigzag type and armchair type edges). Finite graphite

systems having zigzag edges exhibit a special edge state. The corresponding energy bands are almost flat at the Fermi energy, thereby giving a sharp peak in the density of states (DOS) at the Fermi energy. As a result, conduction electrons are localized around the zig-zag edges of nanographites, forming localized magnetic moments. Recently Harigaya [29] has theoretically predicted that the magnetism in nanographites with zigzag edge sites depends on the stacking sequence of nanographites. The antiferromagnetic spin alignment becomes energetically favorable when the adjacent graphene sheets have a A-B type stacking sequence along the c axis, like pristine graphite [30]. The AF short-range order in nanographites may coexist with the superconductivity occurring in Sn sheets even at low T and low H .

5 CONCLUSION

Sn-MG is a quasi-2D superconductor, showing a superconducting transition at $T_c = 3.75$ K for $H = 0$. The H - T diagram of Sn-MG consists of four lines (H_{ag} , H_{gl} , $H_{gl'}$, and H_{al}) separating vortex lattice phase, vortex glass phase, and vortex liquid phase. These lines merge into the multicritical point located at $T^* = 3.4$ K and $H^* = 40$ Oe. The irreversibility lines H_{gl} and $H_{gl'}$ intersect at a critical point at $T'_0 = 2.5$ K and $H'_0 = 160$ Oe. The line H_{gl} has an AT-power law form, while the line $H_{gl'}$ has a GT-power law form. The slow dynamics and nonlinearity in the vortex glass phase is an analogy to that in the spin glass phase observed in 3D Ising spin glasses. Further studies will be required to understanding the nature of the vortex glass phase from measurements of resistivity (the nonlinear relation of current-voltage) and the absorption and dispersion at frequencies ($f \gg 1$ kHz).

Acknowledgements

The work at Binghamton (M.S. and I.S.S.) was supported by the Research Foundation of SUNY-Binghamton (contract number 240-9522A). The work at Osaka (J.W.) was supported by the Ministry of Education, Science, Sports and Culture, Japan [the grant for young scientists (No. 70314375)] and by Kansai Invention Center, Kyoto, Japan.

References

- [1] G. Blatter, M.V. Feigel'man, V.B. Geshkenbein, A.I. Larkin, V.M. Vinokur, Rev. Mod. Phys. 66 (1994) 1125. See also references therein.

- [2] P.L. Gammel, D.A. Huse, D.J. Bishop, in: A.P. Young(Ed), Spin Glasses and Random Fields, World Scientific Publishing, Singapore, 1998, p.299. See also references therein.
- [3] G. Menon, Phys. Rev. B 65 (2002) 104527.
- [4] K.A. Müller, M. Takashige, J.G. Bednorz, Phys. Rev. Lett. 58 (1987) 1143.
- [5] J.R.L. de Almeida, D.J. Thouless, J. Phys. A 11 (1978) 983.
- [6] E. Maxwell, Phys. Rev. 86 (1952) 235.
- [7] M. Gabay, G. Toulouse, Phys. Rev. Lett. 47 (1981) 201.
- [8] J. Walter, H. Shioyama, Phys. Lett. A 254 (1999) 65.
- [9] J. Walter, Adv. Mater. 12, (2000) 31.
- [10] J. Walter, Phil. Mag. Lett. 80 (2000) 257.
- [11] J. Walter, J. Heiermann, G. Dyker, S. Hara, H. Shioyama, J. Catalysis 189 (2000) 449.
- [12] M. Suzuki, I.S. Suzuki, T.Y. Huang, J. Phys.: Condensed Matter 14 (2002) 5583.
- [13] K. Gunnarsson, P. Svedlindh, P. Nordblad, L. Lundgren, H. Aruga, A. Ito, Phys. Rev. Lett. 61 (1988) 754.
- [14] J. Heremans, C.H. Olk, D.T. Morelli, Phys. Rev. B 49 (1994) 15122.
- [15] K. Shibata, T. Nishizuka, T. Sasaki, N. Kobayashi, Phys. Rev. B 66 (2002) 214518. See also references therein.
- [16] U. Welp, J.A. Fendrich, W.K. Kwok, G.W. Crabtree, B.W. Veal, Phys. Rev. Lett. 76 (1996) 4809.
- [17] J.A. Mydosh, Spin glasses: an experimental introduction, Taylor & Francis, London, 1993.
- [18] N.R. Werthamer, E. Helfand, P.C. Hohenberg, Phys. Rev. 147 (1966) 2953.
- [19] I. Didschuns, K. Fleischer, P. Schilbe, N. Esser, W. Richter, K. Luders, Physica C 377 (2002) 89.
- [20] V.N. Vieira, J. Schaf, Physica C 384 (2003) 514.
- [21] V.N. Vieira, J.P. da Silva, J. Schaf, Phys. Rev.B 64 (2001) 094516.
- [22] G.G. Kenning, D. Chu, R. Orbach, Phys. Rev. Lett. 66 (1991) 2923.
- [23] See, for example, J.B. Ketterson, S.N. Song, Superconductivity, Cambridge University Press, Cambridge, 1998.
- [24] V.B. Geshkenbein, V.M. Vinokur, R. Fehrenbacher, Phys. Rev. B 43 (1991) 3748.

- [25] D.G. Steel, J.M. Graybeal, Phys. Rev. B 45 (1992) 12643.
- [26] M. Suzuki, I.S. Suzuki, R. Lee, J. Walter, Phys. Rev. B 66 (2002) 014533.
- [27] M. Fujita, K. Wakabayashi, K. Nakada, K. Kusakabe, J. Phys. Soc. Jpn. 65 (1996) 1920.
- [28] K. Wakabayashi, M. Fujita, H. Ajiki, M. Sigrist, Phys. Rev. B 59 (1999) 8271.
- [29] K. Harigaya, J. Phys. Condensed Matter 13 (2001) 1295.
- [30] T. Enoki, M. Suzuki, M. Endo, Graphite Intercalation Compounds and Applications, Oxford University Press, New York, 2003.